

Different behaviour of magnetic impurities in crystalline and amorphous states of superconductors

To cite this article: Mi-Ae Park *et al* 2002 *Supercond. Sci. Technol.* **15** 1557

View the [article online](#) for updates and enhancements.

Related content

- [The influence of Frenkel defects on the anomalous resistivity and thermopower of dilute CuCr alloys](#)
G Wehr, G Sieber and K Boning
- [SQUID-magnetometer combined with ion implantation](#)
M Hitzfeld, P Ziemann and W Buckel
- [Formation of localized moments in metals: experimental bulk properties](#)
C Rizzuto



IOP | ebooks™

Bringing you innovative digital publishing with leading voices to create your essential collection of books in STEM research.

Start exploring the collection - download the first chapter of every title for free.

Different behaviour of magnetic impurities in crystalline and amorphous states of superconductors

Mi-Ae Park¹, Kerim Savran² and Yong-Jihn Kim^{2,3}

¹ Department of Physics, University of Puerto Rico at Humacao, Humacao, PR 00791, USA

² Department of Physics, Bilkent University, 06533 Bilkent, Ankara, Turkey

Received 30 May 2002

Published 17 October 2002

Online at stacks.iop.org/SUST/15/1557

Abstract

It has been observed that the effect of magnetic impurities in a superconductor is drastically different depending on whether the host superconductor is in the crystalline or the amorphous state. Based on the recent theory of Kim and Overhauser (KO), it is shown that as the system is getting disordered, the initial slope of the T_c depression is decreasing by a factor $\sqrt{\ell/\xi_0}$, when the mean free path ℓ becomes smaller than the BCS coherence length ξ_0 , which is in agreement with experimental findings. In addition, for a superconductor in a crystalline state in the presence of magnetic impurities the superconducting transition temperature T_c drops sharply from about 50% of T_{c0} (for a pure system) to zero near the critical impurity concentration. This *pure limit behaviour* was indeed found by Roden and Zimmermeyer in crystalline Cd. Recently, Porto and Parpia have also found the same *pure limit behaviour* in superfluid He-3 in aerogel, which may be understood within the framework of the KO theory.

1. Introduction

It has been well appreciated among experimentalists that the effect of magnetic impurities in superconductors depends strongly on whether the host superconductor is in the crystalline state or in the amorphous state [1–13]. For instance, the initial slope of the T_c decrease due to magnetic impurities turned out to be not universal but dependent on the sample quality and sample preparation methods. This was not well understood. Recently, Kim and Overhauser (KO) [14] have proposed a theory of magnetic impurity effect on superconductors, which anticipates the above experimental observations. To summarize, they obtained the following results:

- (1) The initial slope of the T_c decrease due to magnetic impurities depends on the superconductor and, therefore, is not a universal constant.
- (2) The reduction of T_c by magnetic impurities is significantly lessened whenever the mean free path ℓ becomes smaller than the BCS coherence length ξ_0 .

The second result, called compensation phenomenon, has been observed by adding non-magnetic impurities [1, 2] and radiation damage [4, 5, 8]. Indeed, Park *et al* [15] showed that the KO theory leads to a good fitting to the experimental data obtained from radiation damage [8]. The first result is not easy to confirm experimentally for the following reasons. First, the initial slopes for the usual low T_c superconductors are not much different. Secondly, it is not easy to control the contents of ordinary and magnetic impurities and the disorder in different superconductors.

In this study we combine the first and the second results to obtain the following result:

- (1) As the system is getting disordered, the initial slope of the T_c depression is decreasing by a factor $\sqrt{\ell/\xi_0}$. (This was not calculated in KO's paper.) This result agrees with the experimental fact that the observed initial decrease of T_c for superconductors as a function of the concentration c of the magnetic ions is larger in the crystalline state than that in the amorphous state of superconductors. In table 1, most of the values from the literature for the initial decrease of T_c for the Zn–Mn system are listed, which shows this behaviour spectacularly. Data are from Falke *et al* [13]. As can be seen,

³ Present address: Department of Physics, University of Puerto Rico, Mayaguez, PR 00681, USA.

Table 1. Values for the initial depression $-(dT_c/dc)_{\text{initial}}$ of the T_c of Zn with different concentrations of Mn. Data are from Falke *et al* [13].

$-(dT_c/dc)_{\text{initial}}$ in (K/at%)	Sample	Reference
170	Bulk	[16] (1964)
315	Bulk	[2] (1966)
>300	Bulk	[17] (1968)
260 (290)	Bulk	[18] (1971)
300	Bulk	[19] (1972)
630	Single crystal	[7] (1975)
215	Thin film	[20] (1967)
285	Thin film	[13] (1973)

the initial slope of the T_c decrease by magnetic impurities is not universal but dependent on the sample quality and sample preparation methods. Note that Zn–Mn alloys show all the Kondo anomalies at low temperatures [21].

On the other hand, Porto and Parpia [22] (and other researchers [23, 24]) have recently found that T_c of superfluid He-3 in aerogel drops suddenly to zero at around 2.7 bar. The discovery has attracted much attention [25, 26]. We point out that this behaviour may be understood in terms of the KO theory. In fact, the KO theory implies that if spin-disorder scattering *only* is taken into account, T_c drops suddenly from about 50% of T_{c0} (for the pure metal) to zero near the critical impurity concentration. This may be called the *pure limit behaviour* [7]. However, KO did not expect the observability of this behaviour in superconductors because the influence of the (neglected) potential scattering from the paramagnetic solutes was believed to be dramatic [14]. This phenomenon was called self-compensation of the paramagnetic impurity effect. In other words, KO thought self-compensation will wash out the *pure limit behaviour*. However, this conclusion is based on the assumption that the coherence length will decrease significantly even for $\ell > \xi_0$, [14] which may not be valid. Whereas, in superfluid He-3 in aerogel, aerogel acts like impurities and decreases the transition temperature without disturbing the liquid state of He-3 significantly. So the *pure limit behaviour* may be easily observable. (It is straightforward to apply the KO theory to p-wave pairing states [27]. In the appendix, the impurity effect on the ABM state is considered within the KO theory. More details will be published elsewhere.)

Another result of this study is about the observability of the *pure limit behaviour* in superconductors:

(2) If the host superconductor in the presence of the magnetic impurities is pure enough for exchange scattering to dominate, then the *pure limit behaviour* may be observable, i.e. T_c drops suddenly from about 50% of T_{c0} (for the pure metal) to zero near the critical impurity concentration. Accordingly, it is desirable to add chemically-similar impurities to the host superconductor with much low T_c .

But, in general, the *pure limit behaviour* in superconductors is hard to observe experimentally due to the potential scattering from the magnetic impurities, and the metallurgical problems related to a very small solubility of magnetic impurities in non-transition metals. Also adding many magnetic impurities may make the host superconductors disordered. Therefore, it is really remarkable that Roden and Zimmermeyer [6] confirmed the *pure limit*

Table 2. Reduction in the T_c of some superconductors by magnetic impurities. Data are from Buckel [10], Wassermann [3] and Schwidtal [30].

Superconductor	Additive	$-dT_c/dc$ in K/at%
Pb	Mn	21 ^a [32], 16 ^b [33]
Sn	Mn	69 ^a [34], 14 ^b [33]
Zn	Mn	315 [2], 285 ^a [13], 343 ^b [35], 630 [7]
Zn	Cr	170 [2], 90–200 [3]
Cd	Mn	44 [20], 5.4 ^a [6]
In	Mn	25 [4], 53 ^a [36], 50 ^b [8], 100 [1]
In	Fe	2.5 [36], 2.0 [37]
La	Gd	5.1 ^a [38], 4.5 ^b [39]

^a Quench-condensed films.

^b Ion implantation at low temperatures.

behaviour, in crystalline cadmium doped with dilute Mn atoms by quench condensation. The reasons for their success seem to be the following: (1) since the T_c of crystalline Cd is so low ($T_c = 0.9$ K), the critical impurity concentration is low ($c_{cr} \sim 0.07$ at% enough not to disturb the crystalline state of Cd), (2) Mn atoms may not lead to strong potential scatterings in Cd. It is well known that sample preparation of thin-film alloys by evaporation on cold substrates (quench condensation) is suitable for producing alloys between otherwise insoluble components. They prepared (micro)crystalline and amorphous cadmium with dilute Mn impurities. Remarkably, they found that a quench-condensed film of cadmium in the microcrystalline state shows an abrupt decrease of the transition temperature near the critical impurity concentration.

In this paper, we use the KO theory to explain the difference of the magnetic impurity effect in crystalline and amorphous states of superconductors. The *pure limit behaviour* in superconductors and the change of the initial slope of the T_c depression due to disorder are investigated. We find a good agreement with the existing experimental data. A brief review of experimental works is given in section 2, while the KO theory is described in section 3. Comparison with various experimental data is given in section 4. In the appendix the KO theory is extended to the p-wave pairing state for superfluid He-3 in aerogel.

2. Magnetic impurity effect in crystalline and amorphous states of superconductors

In this section, the experimental data for the effect of magnetic impurities on the crystalline and amorphous states of superconductors are briefly reviewed. Although there are already a few review articles on magnetic impurity effect in superconductors [28, 29], this topic was not spotlighted before, simply because the experimental data were not understood. Nevertheless, it was observed by many experimentalists that the magnetic impurity effects are different for crystalline and amorphous states of superconductors. To illustrate, the initial decrease of T_c for some superconductors as a function of the concentration c of the magnetic ions is summarized in table 2. The table is from Buckel [10], Wassermann [3] and Schwidtal [30]. It is clear that the initial T_c decrease depends on the sample quality and is not the universal constant suggested

by Abrikosov and Gor'kov [31]. Note that In–Mn [4, 5, 8], Sn–Mn [33], Zn–Mn [13] and Cd–Mn [40] show the Kondo anomalies at low temperatures.

Merriam *et al* [1] were the first who found the difference. They investigated the effect of dissolved Mn on superconductivity of pure and impure In. They observed that the addition of a third element, Pb or Sn, progressively decreases the effect of Mn and eliminates the effect completely when the mean free path is decreased sufficiently enough. In other words, the T_c depression arising from a paramagnetic solute turned out to be mean-free-path dependent. Boato, Gallinaro and Rizzuto [2] confirmed the result. It was also found that T_c depression by transition metal impurities in bulk metals and thin films leads very often to different results [3]. For instance, broad scattering of the experimental $-dT_c/dc$ values was frequently obtained, presumably due to the differences in the degree of disorder. A review was given by Wassermann [3]. On the other hand, Falke *et al* [13] investigated transition temperature depression in quench-condensed Zn–Mn dilute alloy films and compared it with bulk data. Their work gives good support to the equivalence of thin films and bulk material. To put it another way, even though the initial T_c depression caused by magnetic impurities may be different for thin films and bulk material, a magnetic impurity may possess a stable magnetic moment whether it is in thin films or in bulk material. Bauriedl and Heim [4] noted that the reason for the different behaviour of a magnetic impurity in crystalline and disordered materials is lattice disorder. The authors considered annealed In films implanted with 150 keV Mn ions at low temperatures and increased the lattice disorder by pre-implantation of In ions, which led to the variation of the initial T_c depression between 26 K/at% for the crystalline sample and 10 K/at% for the heavily disordered sample. Hitzfeld and Heim [5] reported that the magnetic state of Mn in ion-implanted In–Mn alloys is not so much affected by incorporating oxygen (lattice disorder) but the superconducting properties changes significantly, in agreement with Falke *et al* [13]: $-dT_c/dc$ is changed from 24 to 18 K/at% if oxygen is added. Schlabitzi and Zaplinski [7] reported on the influence of lattice defects on the T_c depression in dilute Zn–Mn single crystals. Their measurements also show a much higher depression of T_c for single crystals than for cold-rolled crystals and quench-condensed films. Hofmann *et al* [8] also observed compensation of the paramagnetic impurity effect as a consequence of radiation damage. Well-annealed In films implanted at low temperatures with Mn ions lead to an initial slope of 50 K/at%, whereas In films irradiated with high fluences of Ar ions before the Mn implantation lead to a slope of 39 K/at%. In addition, 90% of the 2.2 K decrease in T_c caused by Mn implantation was suppressed by an Ar fluence of $2.2 \times 10^{16} \text{ cm}^{-2}$. Habisreuther *et al* [9] reported on an *in situ* low-temperature ion-implantation study of Mn in crystalline β -Ga and amorphous a -Ga films. They found linear T_c decreases in a -Ga films with a slope of 3.4 K/at% and in β -Ga films with a slope of 7.0 K/at%, (i.e., twice as large as in a -Ga). Recently, Chervenak and Valles [11] investigated magnetic impurity effect in ultrathin, homogeneous $\text{Pb}_{0.9}\text{Bi}_{0.1}$ films with $150 \Omega < R_N < 2.2 \text{ k}\Omega$ and $6.0 \text{ K} > T_c > 2.35 \text{ K}$. Here R_N denotes the normal-state sheet resistance. They found that the effect of magnetic impurities on T_c decreases with

increasing disorder for $4 \text{ K} < T_c < 6 \text{ K}$, in agreement with other experiments. Terris and Ginsberg [12] noted the different electron-tunnelling characteristics in superconducting quench-condensed and annealed manganese-doped zinc films.

Furthermore, Roden and Zimmermeyer [6] considered crystalline and amorphous cadmium with dilute Mn atoms. In the first case the initial depression of T_c is $-dT_c/dc = 5.4 \text{ K/at}\%$ and in the second case $-dT_c/dc = 2.65 \text{ K/at}\%$ in accordance with other results. Surprisingly, a sudden drop of T_c in crystalline cadmium near the critical concentration was observed. About 50% of T_{c0} was decreased to zero by adding additional small amounts of Mn atoms in the (micro)crystalline state, which is consistent with the KO theory. Since the transition temperature of pure Cd in the crystalline state is 0.9 K (T_{c0}), the critical Mn impurity concentration is so low ($\sim 0.075 \text{ at}\%$) that the crystalline state is not much disturbed by Mn atoms. Consequently, the *pure limit behaviour* of magnetic impurity effect was observable. Zimmermeyer and Roden [41] also found a similar behaviour in microcrystalline films of lead doped with Mn, but with a peak just before T_c drops to zero suddenly. The critical concentration is $\sim 0.4 \text{ at}\%$. In this case, since the initial T_c depression is not linear as a function of Mn concentration, there seems to be some solubility problem.

3. Theory of Kim and Overhauser

3.1. Ground state wavefunction

For a homogeneous system, the BCS wavefunction is given by [42, 43]

$$\tilde{\phi} = \prod_k (u_k + v_k a_{k\uparrow}^\dagger a_{-k\downarrow}^\dagger) \phi_0 \quad (1)$$

where the operator $a_{k\alpha}^\dagger$ creates an electron in the state ($k\alpha$) (with the energy ϵ_k) when operating on the vacuum state designated by ϕ_0 . Note that $\tilde{\phi}$ is an approximation of ϕ_N ,

$$\begin{aligned} \phi_N = & A[\phi(r_1 - r_2) \cdots \phi(r_{N-1} - r_N) \\ & \times (1 \uparrow)(2 \downarrow) \cdots (N-1 \uparrow)(N \downarrow)] \end{aligned} \quad (2)$$

where

$$\phi(r) = \sum_k \frac{v_k}{u_k} e^{ik \cdot r} \quad (3)$$

and both wavefunctions lead to the same result for a large system. Nevertheless, ϕ_N is more helpful in understanding the underlying physics related to the magnetic impurity effect in superconductors: we are concerned with a bound state of Cooper pairs in a BCS condensate. It should be noted that the (bounded) pair wavefunction $\phi(r)$ and the BCS pair-correlation amplitude $I(r)$ [42] are basically the same for large N :

$$\phi(r) = \sum_k \frac{\Delta_k}{\epsilon_k + E_k} e^{ik \cdot r}, \quad (4)$$

$$I(r) = \sum_k \frac{\Delta_k}{2E_k} e^{ik \cdot r} \sim \Delta K_0 \left(\frac{r}{\pi \xi_0} \right), \quad (5)$$

where

$$E_k = \sqrt{\epsilon_k^2 + \Delta_k^2}. \quad (6)$$

Here K_0 is a modified Bessel function which decays rapidly when $r > \pi\xi_0$.

In the presence of magnetic impurities, BCS pairing must employ degenerate partners which have the exchange scattering (due to magnetic impurities) built in because the strength of exchange scattering J is much larger than the binding energy. This scattered state representation was first introduced by Anderson [44] in his theory of dirty superconductors. Accordingly, the corresponding wavefunctions are

$$\tilde{\phi}' = \prod_n (u_n + v_n a_{n\uparrow}^\dagger a_{n\downarrow}^\dagger) \phi_0 \quad (7)$$

and

$$\phi'_N = A[\phi'(r_1, r_2)\phi'(r_3, r_4) \cdots \phi'(r_{N-1}, r_N)] \quad (8)$$

where

$$\phi'(r_1, r_2) = \sum_n \frac{v_n}{u_n} \psi_{n\uparrow}(r_1) \psi_{n\downarrow}(r_2). \quad (9)$$

Here $\psi_{n\uparrow}$ and $\psi_{n\downarrow}$ denote the exact eigenstate and its degenerate partner, respectively. It is clear from the pair wavefunction $\phi'(r_1, r_2)$ that only the magnetic impurities within ξ_0 of a Cooper pair's centre of mass can diminish the pairing interaction.

3.2. Phonon-mediated matrix element

Now we need to determine the scattered state ψ_n and the phonon-mediated matrix element $V_{nn'}$. The magnetic interaction between a conduction electron at \mathbf{r} and a magnetic impurity (having spin \mathbf{S}), located at \mathbf{R}_i , is given by

$$H_m(\mathbf{r}) = J\mathbf{s} \cdot \mathbf{S}_i v_o \delta(\mathbf{r} - \mathbf{R}_i), \quad (10)$$

where $\mathbf{s} = \frac{1}{2}\sigma$ and v_o is the atomic volume. The scattered basis state which carries the label, $n\alpha = \vec{k}\alpha$, is then

$$\psi_{n\alpha=\vec{k}\alpha} = N_{\vec{k}} \left[e^{i\vec{k}\cdot\vec{r}} \alpha + \sum_{\vec{q}} e^{i(\vec{k}+\vec{q})\cdot\vec{r}} (W_{\vec{k}\vec{q}} \beta + W'_{\vec{k}\vec{q}} \alpha) \right], \quad (11)$$

where,

$$W_{\vec{k}\vec{q}} = \frac{\frac{1}{2}J\bar{S}v_o}{\epsilon_{\vec{k}} - \epsilon_{\vec{k}+\vec{q}}} \sum_j \sin \chi_j e^{i\phi_j - i\vec{q}\cdot\mathbf{R}_j} \quad (12)$$

and,

$$W'_{\vec{k}\vec{q}} = \frac{\frac{1}{2}J\bar{S}v_o}{\epsilon_{\vec{k}} - \epsilon_{\vec{k}+\vec{q}}} \sum_j \cos \chi_j e^{-i\vec{q}\cdot\mathbf{R}_j}. \quad (13)$$

χ_j and ϕ_j are the polar and azimuthal angles of the spin \mathbf{S}_j at \mathbf{R}_j and $\bar{S} = \sqrt{S(S+1)}$. The perturbed basis state for the degenerate partner of (11) is

$$\psi_{\bar{n}\beta=-\vec{k}\beta} = N_{\vec{k}} \left[e^{-i\vec{k}\cdot\vec{r}} \beta + \sum_{\vec{q}} e^{-i(\vec{k}+\vec{q})\cdot\vec{r}} (W_{\vec{k}\vec{q}}^* \alpha - W'_{\vec{k}\vec{q}} \beta) \right]. \quad (14)$$

At each point \vec{r} , the two spins of the degenerate partner become canted by the mixing of the plane wave and spherical-wavelet component. Consequently, the BCS condensate is forced to have a triplet component because of the canting

caused by the exchange scattering. The phonon-mediated matrix element between the canted basis pairs is (to order J^2)

$$V_{nn'} \equiv V_{\vec{k}'\vec{k}} = -V \langle \cos \theta_{\vec{k}'}(\vec{r}) \rangle \langle \cos \theta_{\vec{k}}(\vec{r}) \rangle, \quad (15)$$

where θ is the canting angle. The angular brackets indicate both a spatial average and an impurity average. It is then given by

$$\langle \cos \theta_{\vec{k}}(\vec{r}) \rangle \cong 1 - 2|W_{\vec{k}}|^2, \quad (16)$$

where $|W_{\vec{k}}|^2$ is the relative probability contained in the virtual spherical waves surrounding the magnetic solutes (compared to the plane-wave part). From equations (11)–(13) we obtain

$$|W_{\vec{k}}|^2 = \frac{J^2 m^2 \bar{S}^2 c_m R}{8\pi n \hbar^4}, \quad (17)$$

where c_m is the magnetic solute fraction. Because the pair-correlation amplitude falls exponentially as $\exp(-r/\pi\xi_0)$ [42] at $T = 0$ and as $\exp(-r/3.5\xi_0)$ [45] near T_c , we set

$$R = \frac{3.5}{2} \xi_0. \quad (18)$$

Then one finds

$$\langle \cos \theta \rangle = 1 - \frac{3.5\xi_0}{2\ell_s}, \quad (19)$$

where $\ell_s = v_F \tau_s$ is the mean free path for exchange scattering only.

3.3. BCS T_c equation

The resulting BCS gap equation, near T_c , is given by

$$\bar{\Delta}_{\vec{k}} = - \sum_{\vec{k}'} \frac{V_{\vec{k},\vec{k}'}}{2\bar{\epsilon}_{\vec{k}'}} \frac{\bar{\Delta}_{\vec{k}'}}{2T} \tanh \left(\frac{\bar{\epsilon}_{\vec{k}'}}{2T} \right). \quad (20)$$

Here $\bar{\Delta}_{\vec{k}}$ is the impurity averaged value of the gap parameter whereas $\bar{\epsilon}_{\vec{k}}$ is that of the electron energy. The BCS T_c equation still applies after a modification of the effective coupling constant according to equation (15):

$$\lambda_{\text{eff}} = \lambda \langle \cos \theta \rangle^2, \quad (21)$$

where λ is $N_0 V$. Accordingly, the BCS T_c equation is now,

$$k_B T_c = 1.13 \hbar \omega_D e^{-\frac{1}{\lambda_{\text{eff}}}}. \quad (22)$$

The initial slope is given by

$$k_B (\Delta T_c) \cong - \frac{0.63 \hbar}{\lambda \tau_s}. \quad (23)$$

The factor $1/\lambda$ shows that the initial slope depends on the superconductor and is not a universal constant. For an extended range of solute concentration, KO found

$$\langle \cos \theta \rangle = \frac{1}{2} + \frac{1}{2} \left[1 + 5 \left(\frac{u}{2} \right)^2 \right]^{-1} e^{-2u}, \quad (24)$$

where

$$u \equiv 3.5 \xi_{\text{eff}} / 2\ell_s. \quad (25)$$

We have replaced ξ_0 by the effective coherence length ξ_{eff} which is explained below.

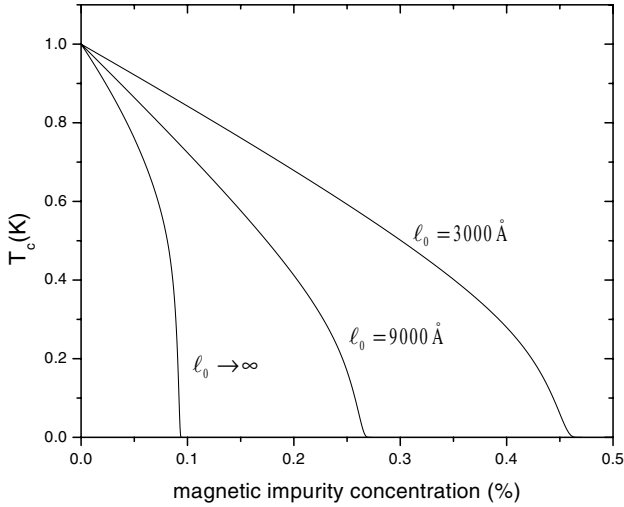


Figure 1. Variation of T_c with magnetic impurity concentration for pure and impure superconductors. ℓ_0 denotes the mean free path for the potential scattering.

3.4. Change of the initial slope of the T_c decrease

When the conduction electrons have a mean free path ℓ which is smaller than the coherence length ξ_0 (for a pure superconductor), the effective coherence length is

$$\xi_{\text{eff}} \approx \sqrt{\ell \xi_0}. \quad (26)$$

For a superconductor which has ordinary impurities as well as magnetic impurities, the total mean free path ℓ is given by

$$\frac{1}{\ell} = \frac{1}{\ell_s} + \frac{1}{\ell_0}, \quad (27)$$

where ℓ_0 is the mean free path for the potential scattering. It is evident from equation (26) that the potential scattering profoundly affects the paramagnetic impurity effect. Consequently, the initial slope of the T_c depression is decreased in the following way:

$$k_B(\Delta T_c) \cong -\frac{0.63\hbar}{\lambda \tau_s} \sqrt{\frac{\ell}{\xi_0}}. \quad (28)$$

This explains the broad scattering of the experimental $-dT_c/dc$ values. In other words, the size of the Cooper pair is reduced by the potential scattering and the reduced Cooper pair sees a smaller number of magnetic impurities. Accordingly, the magnetic impurity effect is partially suppressed, leading to the decrease of the initial slope of the T_c depression.

Figure 1 shows the different behaviour of the T_c depression due to magnetic impurities in the pure crystalline state and in the amorphous or disordered state of superconductors. We used $T_{c0} = 1.0 \text{ K}$, $v_F = 1.5 \times 10^8 \text{ cm s}^{-1}$ and $\omega_D = 250 \text{ K}$. We also assumed the relation between ℓ_s and magnetic impurity concentration c : $\ell_s = 10^5/c(\text{\AA})$. Here c is measured in at%. Since the exchange scattering cross-section is usually 20–200 times smaller than that for the potential scattering, [14] this assumption seems to be reasonable. For the pure crystalline state T_c drops to zero suddenly when T_c is decreased to about 50% of T_{c0} of the pure system, which may be called *pure limit behaviour*. As the mean free path ℓ is decreased due to disorder, the initial T_c depression is weakened and T_c drops to zero more slowly near the critical concentration.

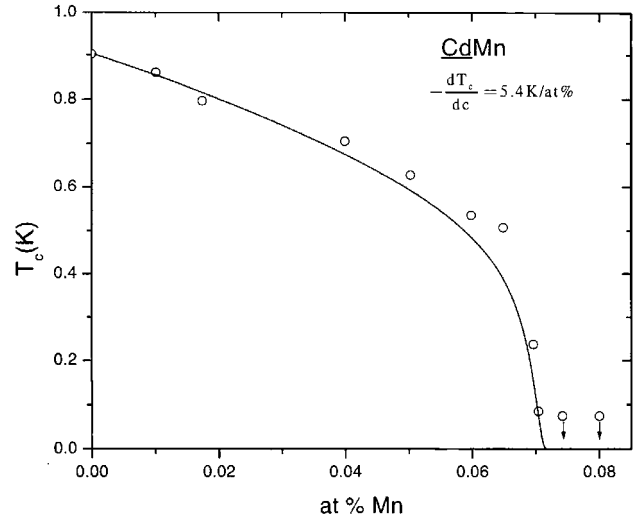


Figure 2. Comparison of the experimental data for CdMn in the microcrystalline state with the KO theory. Data are from Roden and Zimmermeyer [6].

4. Comparison with experiment

The overall agreement between KO theory and the existing experimental data is very good. We focus on the experiments which investigated the difference of the magnetic impurity effect in the pure crystalline state and amorphous or disordered state of superconductors. In cases where mean free paths for the exchange and potential scattering were not available, we consulted other experiments and the well-known normal-state transport properties. Note that exchange coefficients J are $\sim 0.1 \text{ eV}$ and the strength U_0 of the potential scattering is typically $\sim 1 \text{ eV}$ [14, 31]. One should also note the possibility of inhomogeneity in quench-condensed amorphous films [46, 47]. In that case the residual resistivity and the mean free path may not represent well the degree of the disorder in the system. Then our comparison with experimental data is somewhat qualitative.

4.1. Pure limit behaviour: Roden and Zimmermeyer's experiment

Roden and Zimmermeyer [6] prepared alloys of Cd with dilute Mn impurities by quench condensation. Quench condensation produces a variety of states of the alloy: in particular, one can get a microcrystalline and an amorphous state. A quench-condensed film of Cd in the microcrystalline state shows a higher $T_c (=0.9 \text{ K})$ than the bulk material ($T_c = 0.55 \text{ K}$) and a further increase of $T_c (=1.15 \text{ K})$ is obtained in the amorphous state. An amorphous Cd film was obtained by adding Cu atoms. Like other non-transition metals deposited in an ordinary high-vacuum system, quench-condensed Cd film is crystalline with small crystallites [46].

Now we compare the KO theory with Roden and Zimmermeyer's experiment. Figure 2 shows T_c versus magnetic impurity concentration c in the microcrystalline CdMn. The solid line is a theoretical curve obtained from equation (22). The transition temperature T_{c0} of pure Cd in this state is 0.9 K . While the initial depression of T_c is linear in c with a value of $-dT_c/dc = 5.4 \text{ K/at\%}$, above

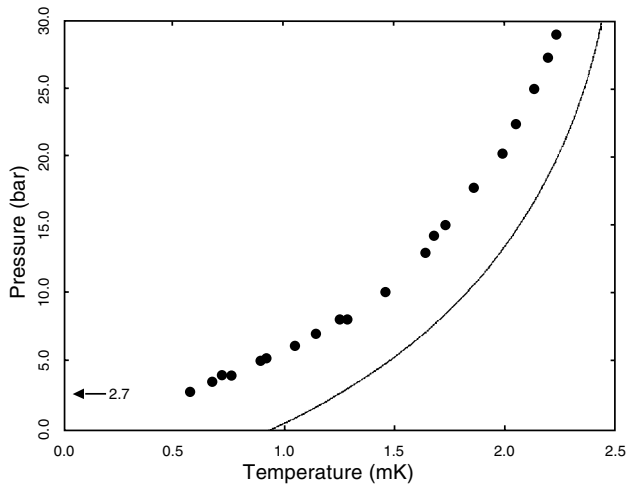


Figure 3. The superfluid transition temperature at various pressures. No superfluid was detected below 2.7 bars. Data are from Porto and Parpia [22].

0.05% the depression becomes much more stronger than linear, which agrees with the KO theory. Arrows denote that no superconductivity was found up to 70 mK. For theoretical fitting we used $T_{c0} = 0.904$ K, $\omega_D = 209$ K and $v_F = 1.62 \times 10^8$ cm s $^{-1}$ [48]. We emphasize that there is no free parameter. But, in the absence of experimental data we assumed $\ell_s = 9 \times 10^5/c(\text{\AA})$, which is reasonable since $J \sim 0.1$ eV. As can be seen, the agreement between the experimental data and the theoretical curve is very good.

It is of interest to compare *pure limit behaviours* in superconductors and superfluid He-3 in aerogel [22–26]. Porto and Parpia [22] reported measurement of the transition temperature of He-3 confined within 98.2% open aerogel. They observed that T_c is suppressed strongly and drops suddenly to zero at 2.7 bars. Figure 3 shows the superfluid transition temperature of He-3 in aerogel at various pressures. This behaviour may also be understood in terms of the KO theory. In the appendix, we apply the KO theory to the ABM state and show that the same *pure limit behaviour* follows for the p-wave pairing states with (ordinary) impurities.

Figure 4 shows T_c versus c for the amorphous CdCuMn. The solid line was obtained from equations (22) and (26). The decrease of T_c for smaller c is again linear but with a much lower $-dT_c/dc = 2.65$ K/at%. In the amorphous state T_{c0} is about 1.18 K. Since the residual resistivity data are not available, we assumed that the mean free path for the potential scattering is $\ell_0 = 4500$ Å. This value is a little bit higher than that expected in homogeneous disordered systems. Note that amorphous Cd films show considerably rounded transition curves which indicate inhomogeneity in samples [46]. We used the same values for ω_D and v_F as in figure 2. Again we find a good fit to the experimental data.

4.2. Change of the initial slope of the T_c depression

Schlabitz and Zaplinski [7] reported measurements of the T_c depression of ZnMn single crystals. In particular, they investigated the influence of lattice defects on the T_c depression in dilute ZnMn single crystals. They demonstrated linear behaviour up to a concentration of 10 ppm with a slope of

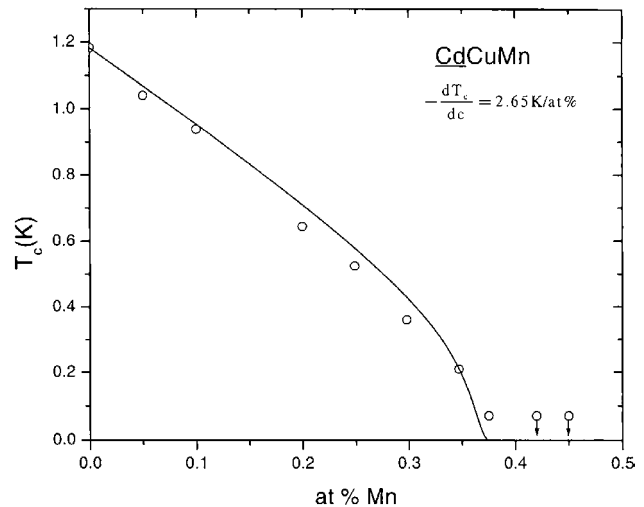


Figure 4. Comparison of the experimental data for CdMn in the amorphous state with the KO theory. Data are from Roden and Zimmermeyer [6].

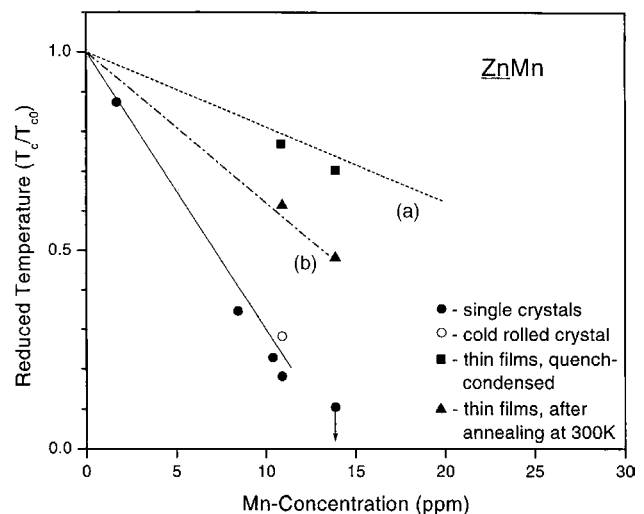


Figure 5. Reduced transition temperature versus Mn concentration for ZnMn. The solid line represents the theoretical curve obtained from equation (29). Line (a): data of thin films from [13], line (b): data of cold-rolled bulk material from [2] and [18]. Data are from Schlabitz and Zaplinski [7].

630 K/at%. This value is twice that of other measurements. As a result, they suggested that the T_c depression can be enhanced strongly by eliminating the lattice defects.

Figure 5 shows the reduced transition temperature, T_c/T_{c0} , as a function of Mn concentration for ZnMn samples. The dashed lines, taken from the other measurements [13], give the T_c depression of: (a) quench-condensed films, and (b) cold-rolled bulk material. The filled points represent the T_c values of the ZnMn single crystals. The filled squares are the data of quench-condensed thin films, while the filled triangles are the data of quench-condensed thin films after annealing at 300 K for 14 h. Since annealing leads to an increased order of the lattice [46], it is clear that the initial slope of the T_c decrease is decreasing as the system is getting disordered.

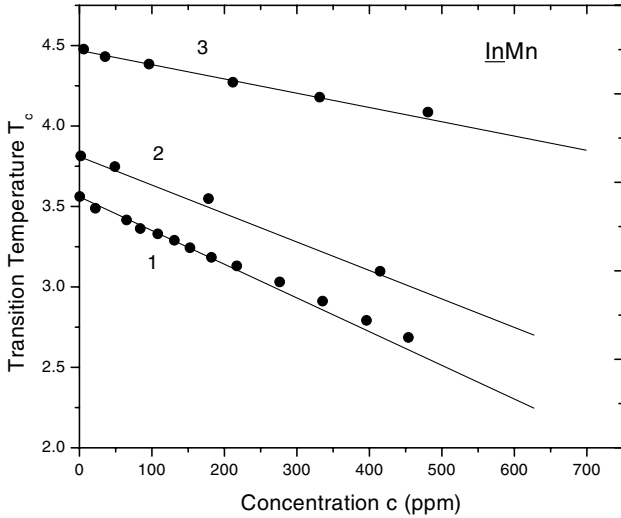


Figure 6. Calculated transition temperatures for implanted InMn alloys. Increasing lattice disorder from 1 to 3 has been produced by pre-implantation of In ions: (1) 0 ppm, (2) 2660 ppm, (3) 18 710 ppm. Data are from Bauriedl and Heim [4].

The solid line is the theoretical curve obtained from the initial slope, $-dT_c/dc = 630 \text{ K/at\%}$ with $T_{c0} = 0.9 \text{ K}$:

$$k_B T_c \cong k_B T_{c0} - \frac{0.63\hbar}{\lambda\tau_s}. \quad (29)$$

This expression agrees very well with the exact BCS T_c equation, equation (22), up to 25% of the critical impurity concentration. The dashed lines (a) and (b) can also be reproduced from the theoretical formula, equation (28),

$$k_B T_c \cong k_B T_{c0} - \frac{0.63\hbar}{\lambda\tau_s} \sqrt{\frac{\ell}{\xi_0}}, \quad (30)$$

for the initial T_c depression in the disordered state of superconductors with (a) $\ell = 3390 \text{ \AA}$, $T_{c0} = 1.51 \text{ K}$ [13] and (b) $\ell = 7520 \text{ \AA}$, $T_{c0} = 0.83 \text{ K}$ [13], respectively. Here T_{c0} values are the experimental results [13]. Note that the quench-condensed amorphous Zn films also show significantly rounded transition curves [46], which explains a somewhat larger value for the mean free path of curve (a). But for curve (b) our mean free path value is reasonable compared to dilute ZnMn alloys data [2, 21]. Therefore, the change of the initial slope of the T_c decrease may be explained in terms of the change of the Cooper pair size caused by the disorder. We used $\omega_D = 327 \text{ K}$ and $v_F = 1.82 \times 10^8 \text{ cm s}^{-1}$ [48]. The sudden drop of T_c near the critical concentration is not pronounced though, presumably because of the smallness of the critical concentration. Since there are not many magnetic impurities in the Zn matrix, the distribution of Mn may be atomically disperse but macroscopically inhomogeneous. Then, the *pure limit behaviour* may not be observable.

Bauriedl and Heim [4] investigated the influence of lattice disorder on the magnetic properties of InMn alloys. Crystalline In films were implanted by Mn ions. The amount of lattice disorder was changed in a very controlled way by pre-implantation of indium with its own ions, which was very effective in producing disordered films.

Figure 6 shows the transition temperatures for InMn alloys with increasing lattice disorder from 1 to 3 by pre-implantation of In^+ ions: (1) 0 ppm; (2) 2660 ppm;

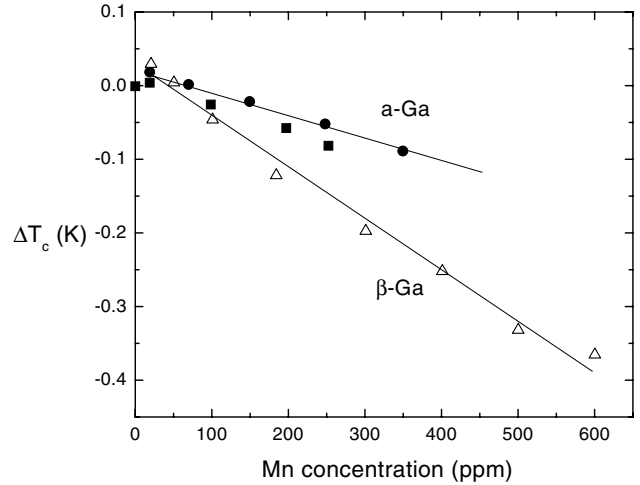


Figure 7. Calculated changes of the superconducting transition temperature ΔT_c versus impurity concentration for Mn-implanted amorphous a -Ga and crystalline β -Ga. Data are from Habisreuther *et al* [9].

(3) 18 710 ppm. These ions have an intensive damaging effect, resulting in an increased residual resistivity and an enhanced transition temperature T_{c0} [5]. Note that the initial slope decreases as the system is more disordered. The solid lines are the theoretical results from equation (28) with (1) $\ell = 1050 \text{ \AA}$, (2) $\ell = 700 \text{ \AA}$ and (3) $\ell = 150 \text{ \AA}$. Since the residual resistivity of sample 1 is about $\sim 0.62 \mu\Omega \text{ cm}$ ($\pm 20\%$) [8], we can obtain $\ell = 1050 \text{ \AA}$. The mean free paths for samples 2 and 3 are also consistent with the related experiment [49]. It is necessary to emphasize that the change of the initial slope due to the enhanced T_{c0} (equation (23)) is not enough to explain the experimental data. We assumed the initial slope $-dT_c/dc = 53 \text{ K/at\%}$ for a pure system [36]. We also used $\omega_D = 108 \text{ K}$ and $v_F = 1.74 \times 10^8$ [48]. We find good agreements between theory and experiment.

Finally, Habisreuther *et al* [9] investigated the magnetic behaviour of Mn in crystalline β -Ga and amorphous a -Ga films. Mn ions were implanted at low temperature ($T < 10 \text{ K}$). The amorphous a -Ga exhibits a rather high transition temperature with typical values between 8.1 and 8.4 K, while the crystalline β -Ga phase shows a transition temperature of $T_c = 6.3 \text{ K}$.

Figure 7 shows changes in the superconducting transition temperature ΔT_c produced by Mn implantation into amorphous a -Ga films and crystalline β -Ga films as a function of the impurity concentrations. Note that the initial slope 3.4 K/at\% in amorphous a -Ga is about half of that (7.0 K/at\%) in crystalline β -Ga films. Theoretical curves represent the initial slope formulae, equations (23) and (28) with $-dT_c/dc = 7 \text{ K/at\%}$, $\ell = \infty$ for β -Ga, and with $-dT_c/dc = 7 \text{ K/at\%}$, $\ell = 600 \text{ \AA}$ for a -Ga. We used $\omega_D = 320 \text{ K}$ and $v_F = 1.91 \times 10^8 \text{ cm s}^{-1}$ [48]. A good fit to the experimental data is obtained.

5. Discussion

It is clear that a systematic experimental study of the effect of magnetic impurities in crystalline and amorphous

superconductors is necessary. In particular, the *pure limit behaviour* in a crystalline state of superconductors and the change of the initial slope due to disordering need more careful studies. This study may shed new light on the old question of whether a transition metal impurity possesses a stable local magnetic moment within a metallic host [50].

The observed *pure limit behaviour* in the superfluid He-3 in aerogel may be compared with that in crystalline superconductors including Cd. In the superfluid He-3 aerogel does not disturb the liquid state of He-3 significantly, whereas in superconductors, adding magnetic impurities may damage the crystalline state of the superconductors, resulting in a difficulty in observing the *pure limit behaviour*.

In our theoretical fitting in most cases we guessed the mean free path ℓ because the experimental residual resistivity data were not available. If the residual resistivity is given, the mean free path ℓ can be determined from the Drude formula. It is interesting to note that the initial T_c depression also provides a way to estimate the mean free path ℓ in disordered superconductors except inhomogeneous amorphous samples.

In this study, weak-coupling BCS theory is used to investigate the effect of magnetic impurities in superconductors. It is straightforward to extend this study to the strong-coupling theory [51, 52]. To do that, pairing of the degenerate scattered state partners is also needed [53]. The result will then basically be the same as that of the weak-coupling theory. More details will be published elsewhere. Actually Jarrel [54] numerically calculated from the Eliashberg equations the initial depression of the T_c due to a small concentration of magnetic impurities and found that the initial depression depends strongly upon the electron–phonon coupling constant λ , in agreement with the KO theory.

6. Conclusion

The effect of magnetic impurities in crystalline and amorphous states of superconductors has been studied theoretically. The *pure limit behaviour* in crystalline Cd observed by Roden and Zimmermeyer and the decrease of the initial slope of the T_c depression due to disorder have been explained. In particular, the initial slope of the T_c decrease is decreasing by a factor $\sqrt{\ell/\xi_0}$ as the system is getting disordered. We suggest that a more systematic experimental investigation is necessary for studying the different behaviour of the magnetic impurities in crystalline and amorphous superconductors.

Acknowledgments

YJK is grateful to Professor C Bulutay for discussions. M Park thanks the FOPI at the University of Puerto Rico-Humacao for release time.

Appendix

The purpose of this appendix is to show that the theory of Kim and Overhauser (KO) is also applicable to the effect of (ordinary) impurities on p-wave pairing states. Note that recent experimental studies of Superfluid He-3 in aerogel

[22–26] have shown the same *pure limit* behaviour which may be understood by a slight variation of the KO theory.

For simplicity, we consider the ABM state [27]

$$\Delta_{\mathbf{k}}^{\uparrow\uparrow} = \Delta_0 \sin \theta_{\mathbf{k}} e^{i\phi_{\mathbf{k}}}, \quad \Delta_{\mathbf{k}}^{\downarrow\downarrow} = \Delta_0 \sin \theta_{\mathbf{k}} e^{-i\phi_{\mathbf{k}}}, \quad (31)$$

where $\theta_{\mathbf{k}}$ and $\phi_{\mathbf{k}}$ are the polar and azimuthal angles of \mathbf{k} . (The other p-wave pairing states such as BW state and polar state will be considered elsewhere.) For a p-wave superconductor, the pairing interaction $V_{\mathbf{k},\mathbf{k}'}$ for the plane-wave state is taken to be

$$V_{\mathbf{k},\mathbf{k}'} = \int e^{i(\mathbf{k}-\mathbf{k}')\cdot\mathbf{r}} V(\mathbf{r}) d^3\mathbf{r} = -3V_1(\hat{\mathbf{k}} \cdot \hat{\mathbf{k}}'), \quad (32)$$

where $\hat{\mathbf{k}}$ is the unit vector parallel to \mathbf{k} . The resulting BCS gap equation, near T_c , is

$$\Delta_{\mathbf{k}} = 3V_1 \sum_{\mathbf{k}'} \hat{\mathbf{k}} \cdot \hat{\mathbf{k}}' \frac{\Delta_{\mathbf{k}'}}{2\epsilon_{\mathbf{k}}} \tanh\left(\frac{\epsilon_{\mathbf{k}'}}{2T}\right). \quad (33)$$

(Actually we should divide equation (33) by a factor of 2 to avoid counting the pair of states ($\mathbf{k} \uparrow, -\mathbf{k} \uparrow$) twice [27]. It may be taken into account by rescaling the pairing potential.) Substituting equation (31) into equation (33), one finds the T_c equation

$$T_c = 1.13\epsilon_c e^{-1/N_0 V_1}, \quad (34)$$

where ϵ_c is the cut-off energy and N_0 is the density of states at the Fermi level.

In the presence of impurities, the pairing matrix element $V_{nn'}$ between scattered basis pairs ($\psi_{n\alpha}, \psi_{\bar{n}\alpha}$) and ($\psi_{n'\alpha}, \psi_{\bar{n}'\alpha}$) is given by

$$V_{nn'} = \int \int d\mathbf{r}_1 d\mathbf{r}_2 \psi_n^*(\mathbf{r}_1) \psi_{\bar{n}'}^*(\mathbf{r}_2) V(|\mathbf{r}_1 - \mathbf{r}_2|) \psi_{\bar{n}}(\mathbf{r}_2) \psi_n(\mathbf{r}_1). \quad (35)$$

Here $\psi_{\bar{n}}$ denotes the time-reversed state of ψ_n . The scattering potential from the impurities can be represented by

$$U(\mathbf{r}) = \sum_i u \delta(\mathbf{r} - \mathbf{R}_i). \quad (36)$$

$\{\mathbf{R}_i\}$ is the impurity sites. Then the scattered basis which carries the label $\mathbf{k}\alpha$ is given by

$$\psi_{\mathbf{k}\alpha} = N_{\mathbf{k}} \left[e^{i\mathbf{k}\cdot\mathbf{r}} + \sum_{i,\mathbf{q}} \frac{u}{\epsilon_{\mathbf{k}} - \epsilon_{\mathbf{k}+\mathbf{q}}} e^{-i\mathbf{q}\cdot\mathbf{R}_i} e^{i(\mathbf{k}+\mathbf{q})\cdot\mathbf{r}} \right] \alpha. \quad (37)$$

Upon employing equations (32), (35) and (37), we obtain

$$V_{\mathbf{k},\mathbf{k}'} = -3V_1(\hat{\mathbf{k}} \cdot \hat{\mathbf{k}}') N_{\mathbf{k}}^2 N_{\mathbf{k}'}^2. \quad (38)$$

Now we need to determine the normalizing factor $N_{\mathbf{k}}^2$

$$N_{\mathbf{k}}^2 = \frac{1}{1 + |W_{\mathbf{k}}|^2}, \quad (39)$$

where $|W_{\mathbf{k}}|^2$ is the relative probability contained in the virtual spherical waves surrounding the impurities. As in s-wave superconductors with magnetic impurities, in calculating $|W_{\mathbf{k}}|^2$, we cut off the radial integral at $R = 3.5\xi_0/2$ near T_c . Consequently, one finds the normalizing factor

$$N_{\mathbf{k}}^2 = \frac{1}{1 + 3.5\xi_0/4\ell}, \quad (40)$$

and the reduced pairing matrix element,

$$V_{\mathbf{k},\mathbf{k}'} = -3V_1(\hat{\mathbf{k}} \cdot \hat{\mathbf{k}}') \left[1 + \frac{3.5\xi_0}{\ell} \right]^{-2}, \quad (41)$$

where ℓ is the mean free path. The T_c equation is now,

$$T_c = 1.13\epsilon_c e^{-1/N_0V_1[1+(3.5\xi_0/4\ell)]^{-2}}. \quad (42)$$

It is interesting to note that this equation shows the *pure limit behaviour* as in magnetic impurity effect on s-wave superconductors (compare equations (42) and (22)). It is noteworthy that the d-wave pairing states also exhibit the *pure limit behaviour* in the presence of ordinary impurities [55]. More details will be published elsewhere.

References

- [1] Merriam M F, Liu S H and Seraphim D P 1964 *Phys. Rev.* **136** A17
- [2] Boato G, Gallinaro G and Rizzuto C 1966 *Phys. Rev.* **148** 353
- [3] Wassermann E 1969 *Z. Phys.* **220** 6
- [4] Bauriedl W and Heim G 1977 *Z. Phys. B* **26** 29
- [5] Hitzfeld M and Heim G 1979 *Solid State Commun.* **29** 93
- [6] Roden B and Zimmermeyer G 1976 *J. Low Temp. Phys.* **25** 267
- [7] Schlabitz W and Zaplinski P 1975 *Proc. of 14th Int. Conf. Low Temp. Phys. (Helsinki, 1975)* vol 3 p 452
- [8] Hofmann A, Bauriedl W and Ziemann P 1982 *Z. Phys. B* **46** 117
- [9] Habisreuther T, Miehle W, Plewnia A and Ziemann P 1992 *Phys. Rev. B* **46** 14566
- [10] Buckel W 1991 *Superconductivity: Fundamentals and Applications* (Weinheim: VCH) p 212
- [11] Chervenak J A and Valles J M Jr 1995 *Phys. Rev. B* **51** 11977
- [12] Terris B D and Ginsberg D M 1984 *Phys. Rev. B* **29** 2503
- [13] Falke H, Jablonski H P, Kästner J and Wassermann E F 1973 *Z. Phys.* **259** 135
- [14] Kim Yong-Jihn and Overhauser A W 1994 *Phys. Rev.* **49** 15799
- [15] Park Mi-Ae, Lee M H and Kim Yong-Jihn 1998 *Physica C* **306** 96
- [16] Boato G, Gallinaro G and Rizzuto C 1964 *Rev. Mod. Phys.* **36** 162
- [17] Martin D L 1968 *Phys. Rev.* **167** 640
- [18] Smith W 1971 *J. Low Temp. Phys.* **5** 683
- [19] Sanchez H 1972 *Thesis* Rutgers University, New Brunswick, NJ
- [20] Hedgcock F T and Rizzuto C 1966 *Phys. Lett. A* **24** 17
- [21] Ford P J, Rizzuto C and Salamoni C 1972 *Phys. Rev. B* **6** 1851
- [22] Porto J V and Parpia J M 1995 *Phys. Rev. Lett.* **74** 4667
- [23] Sprague D T, Haard T M, Kycia J B, Rand M R, Lee Y, Hamot P J and Halperin W P 1995 *Phys. Rev. Lett.* **75** 661
- [24] Matsumoto K, Porto J V, Pollack L, Smith E N, Ho T L and Parpia J M 1997 *Phys. Rev. Lett.* **79** 253
- [25] Sprague D T, Haard T M, Kycia J B, Rand M R, Lee Y, Hamot P J and Halperin W P 1996 *Phys. Rev. Lett.* **77** 4568
- [26] Golov A, Porto J V and Parpia J M 1998 *Phys. Rev. Lett.* **80** 4486
- [27] Leggett A J 1975 *Rev. Mod. Phys.* **47** 331
- [28] Maple M B 1976 *J. Appl. Phys.* **9** 179
- [29] Jensen M A and Suhl H 1966 *Magnetism: A Treatise on Modern Theory and Materials* ed G T Rado and H Suhl, vol IIB (New York: Academic) p 183
- [30] Schwidtal K 1960 *Z. Phys.* **158** 563
- [31] Abrikosov A A and Gor'kov L P 1961 *Zh. Eksp. Teor. Fiz.* **39** 1781 (Engl. Transl. 1961 *Sov. Phys.-JETP* **12** 1243)
- [32] Barth N 1957 *Z. Phys.* **148** 646
- [33] Buckel W, Dietrich M, Heim G and Kessler J 1971 *Z. Phys.* **245** 283
- [34] Schertel A 1951 *Phys. Verh.* **2** 102
- [35] Ziemann P 1983 *Festkörperprobleme* **23** 93
- [36] Opitz W 1955 *Z. Phys.* **141** 263
- [37] Reif F and Woolf M A 1962 *Phys. Rev. Lett.* **9** 315
- [38] Matthias B T, Suhl H and Corenzwit E 1958 *Phys. Rev. Lett.* **1** 92
- [39] Schwidtal K 1962 *Z. Phys.* **169** 564
- [40] Hedgcock F T, Mahajan S N and Rizzuto C 1968 *J. Appl. Phys.* **39** 851
- [41] Zimmermeyer G and Roden B 1976 *Z. Phys. B* **24** 377
- [42] Bardeen J, Cooper L N and Schrieffer J R 1957 *Phys. Rev.* **108** 1175
- [43] de Gennes P G 1966 *Superconductivity of Metals and Alloys* (New York: Benjamin) ch 4
- [44] Anderson P W 1959 *J. Phys. Chem. Solids* **11** 26
- [45] Anderson P W and Morel P 1961 *Phys. Rev.* **123** 1911
- [46] Granqvist C G and Claeson T 1973 *J. Low Temp. Phys.* **10** 735
- [47] Belevtsev B I 1990 *Sov. Phys.-Usp.* **33** 36
- [48] Kittel C 1976 *Introduction to Solid State Physics* (New York: Wiley) chs 5 and 6
- [49] Bauriedl W, Heim G and Bukel W 1976 *Phys. Lett. A* **57** 282
- [50] Kapoor J, Andres J, Mezei F, Li Y, Polaczyk C, Riegel D, Brewer W D, Beck E, Legoas S B and Frota-Pessoa S 1996 *Phys. Rev. Lett.* **77** 2806
- [51] Eliashberg G M 1960 *Zh. Eksp. Teor. Fiz.* **38** 966 (Engl. Transl. 1960 *Sov. Phys.-JETP* **11** 696)
- [52] McMillan W L 1968 *Phys. Rev.* **167** 331
- [53] Kim Yong-Jihn 1996 *Mod. Phys. Lett. B* **10** 555
- [54] Jarrel M 1990 *Phys. Rev. B* **41** 4815
- [55] Park M-A, Lee M H and Kim Y-J 1997 *Mod. Phys. Lett.* **11** 719